

Penrose Matching Rules from Realistic Potentials in a Model System

Sejoon Lim, M. Mihalkovič, [†] and C. L. Henley [‡]

Dept. of Physics, Cornell University, Ithaca NY 14853-2501 USA

(–, 2007)

We exhibit a toy model of a binary decagonal quasicrystal of composition $\text{Al}_{80.1}\text{Co}_{19.9}$ – closely related to actual structures – in which realistic pair potentials yield a ground state which appears to perfectly implement Penrose’s matching rules, for Hexagon-Boat-Star (HBS) tiles of edge 2.45 Å. The second minimum of the potentials is crucial for this result.

1 Introduction

After the first couple years of quasicrystal papers, and especially after the discovery of long-range-ordered equilibrium quasicrystals, theorists began to address their stabilisation. But this was mostly in terms of abstract tilings – with inter-tile matching rules (as in Penrose’s tiling), or without (as in the random-tiling models); it was implicitly understood that the tiles’ interactions were induced by those of the atoms. Only towards 1990 did people begin to ask *which* interatomic potentials actually favored specific (hopefully realistic) quasicrystal atomic structures [1–4]

Two competing scenarios emerged for the origins of quasicrystal long-range-order. The matching-rule model posits that atomic interactions implement something like Penrose’s arrows: then there exists an ideal quasicrystal structure (in analogy to ideal crystal structures). This paradigm was esthetically attractive, since it would imply (i) mathematically beautiful symmetries under “inflation” by powers of $\tau \equiv (1 + \sqrt{5})/2$ with interesting consequences for physical properties; (ii) special conditions on the atomic structures when represented as a cut through a higher-dimensional space. [5]

The random-tiling scenario, on the other hand, posits that long-range order is emergent, [6, 7] with the quasicrystal phase well represented as a high-entropy ensemble of different tile configurations. This had an esthetic advantage in the sense of Occam’s razor, in demanding fewer coincidences from the interactions. Furthermore, the known structures appeared to be made from highly symmetrical clusters, which tends to imply random-tiling type interactions (matching rule “markings” always entail a partial spoiling of the tiles’ symmetries).

In the case of icosahedral quasicrystals, the random-tiling scenario seems to be the most plausible. First of all, no simple matching rules are known [5, 8]. More importantly, diffraction experiments have shown diffuse $1/|q|^2$ tails around Bragg peaks which are well fitted by the quasicrystal elastic theory with its “perp” space displacements complementary to the usual kind [9]; such gradient-squared elasticity is not expected in matching-rule based models.

For decagonal quasicrystals, however, the basis for a random-tiling description has been weaker. It is much easier to implement matching rules from local interactions – particularly for the Penrose pattern, as it is rigorously known that other (“local isomorphism”) classes of decagonal pattern demand longer-range interactions in order to force the correct structure [10] or cannot stabilise an ideal quasicrystal [11]. Furthermore, a three-dimensional decagonal random-tiling theory is required – only extensive entropy can stabilise a bulk system [7] – but the theory for stacked decagonal random tilings was never completed [12]. As to experiments, the $1/|q|^2$ tails have not been observed in decagonals, whereas it is claimed (from high-

[†] Also Institute of Physics, Slovak Academy of Sciences, Dubravská cesta 9, 84511 Bratislava, Slovakia (permanent address).

[‡] Corresponding author. Email: clh@ccmr.cornell.edu

resolution electron microscopy) that extreme regularity is seen even in very thin slices (in the random-tiling case, regularity is expected only from averaging over some thickness).

It has been so difficult to distinguish the scenarios experimentally that, for more than a decade, we (M.M., C.L.H, and also M. Widom) have pursued a program to understand the quasicrystal structure from the atomic scale upwards, using effective pair potentials in Al-Ni-Co alloys at both the Ni-rich [13] and Co-rich [14,15] ends. (These turned out to approximate the structural energy quite well, as calibrated against many ab-initio computations). Our recipe for approaching the decagonal ground-state structure [13–15] took as inputs only the two (quasi)lattice constants and the densities of all species as measured experimentally. In our initial “unconstrained” Monte Carlo simulation the atoms hop as a lattice gas [16] on discrete, properly placed candidate sites (see [13,14]. As in [18], our simulation selects the *lowest* energy configuration visited during the run. The resulting low-energy configurations show characteristic structural motifs which, in subsequent stages, are made into decoration *rules* for simulations using reduced degrees of freedom in larger systems.

To our surprise, this framework – for a particular Al-Co composition – implemented a perfect Penrose tiling. In this paper, we explain how this order develops and suggest why it follows from our potentials.

2 Simulations and results

Our model simply consists of Al and Co atoms allowed to have any of the discrete configurations in our initial stage, with the Al density somewhat higher than in real Al-TM decagonals. We used the same “GPT” potentials [17] as in [13] and [14]. Following our standard recipe, [13,14], the first stage of our exploration was an “unconstrained” lattice-gas simulation in Penrose rhombi with edge $a_R \equiv 2.455 \text{ \AA}$ (this is the quasilattice constant found in the real decagonals and their approximants). We have two *independent* layers, separated by $c/2 \equiv 2.04 \text{ \AA}$ (as real decagonals have two layers per stacking period c , to a first approximation). A run typically cooled from $\beta = 1$ to $\beta = 10$ (we will always write β in units of eV^{-1}) with 10^5 trial swaps per swappable atom pair (both neighbor and long-range swaps). In addition, tile rearrangements (“flips”) are allowed, a total of 2000 per flippable pair during the run.

The result is shown in Fig. 1(a). The atoms have organised themselves into an essentially perfect “hexagon-boat-star” (HBS) tiling with edge $a_R = 2.455 \text{ \AA}$. The vertices of this “2.45-HBS” tiling have Al atoms alternating in layer, and each tile has exactly one Co atom on the interior vertex (if the HBS tiles were decomposed into rhombi), in the *same* layer as the Al atoms connected to it by a 2.455 \AA edge. Recall that HBS tiles are formed by merging three, four, or five Penrose rhombi along their edges with double-arrows, but a generic HBS tiling need not satisfy the single-arrow rule.

Furthermore, at the inflated scale $\tau a_R \approx 3.97 \text{ \AA}$, the Co atoms themselves form the vertices (alternating in layer) of a perfect “4.0-HBS” tiling. But so far, these behaviours are quite typical of *all* Al-TM alloys near a quasicrystal-forming composition. A noteworthy but not crucial feature is that a 2.45-HBS vertex site becomes vacant (rather than have Al) whenever it has no Co neighbors [i.e. where surrounded by a Star tile of the 4.0-HBS tiling; this is seen at three places in Fig. 1(a), last panel]. Since the tiles in a Penrose tiling have number ratios $\tau : 1 : 1/\sqrt{5}$ for H:B:S, the densities of atoms per rhombus work out to be $\frac{1}{2}(9 + 1/\sqrt{5})\tau^{-3}$ and $\tau^{-1}/\sqrt{5}$ for Al and Co respectively, giving a rather Al-rich ideal stoichiometry $\text{Al}_{80.1}\text{Co}_{19.9}$, and a reasonable number density $0.0697/\text{\AA}^3$.

The unique and crucial properties of our model’s composition are

- 1 the interiors of the HBS tiles have unique decorations with one interior Al per Hexagon, and two each per Boat or Star, always in a different layer than the central Co and separated by a_R/τ in projection.
- 2 the 2.45-HBS tiling (and perforce its inflation, the 4.0-HBS tiling) obey the Penrose matching rules.¹

It sometimes happens that interactions merely force a supertiling [13] which at larger scales is random, but in a small system spuriously looks like (the approximant of) a quasiperiodic tiling. Therefore, adapting

¹There are four violations per cell necessitated by the periodic boundary conditions, and a few more violations that we ascribe to incomplete minimisation. The energy correlates with the number of violations.

the second stage from our general recipe [13, 14], we ran a second “constrained” simulation: the allowed configurations here are not a lattice gas of atoms, but arbitrary (random) 2.45-HBS tilings. The tiles’ deterministic decorations deviate from the unconstrained results only in that we do *not* change Al \rightarrow vacancy at the vertices where five fat rhombi come together. Also, one of the natural rearrangements in the HBS tiling is BB \leftrightarrow HS which changes the number of Al atoms; hence, it was necessary to implement a grand-canonical simulation so the average Al content is controlled by a chemical potential. (The Co content, however, is fixed for a given simulation cell.)

The “constrained” results are shown in Fig. 1(b): a perfect Penrose tiling is still obtained in a cell τ^4 larger. Most decisively, when the atom positions are lifted into the “perpendicular” space of this tiling [Fig. 1(c)], they form perfect occupation domains, within the “pixels” induced by the use of a periodic approximant. The perfect Penrose pattern persists for chemical potentials in the surprisingly wide range -1.55 to -2.05 eV.

3 Potentials and evolution of order in the model

The excellent order depends on special properties typical of pair potentials for Al-TM alloys. These have strong Friedel oscillations as a function of the interatomic spacing; the second (even third) wells make crucial contributions to deciding the structure. The first-neighbor distances most compatible with the constraint of our underlying 2.45Å tiles are $a_R \approx 2.45\text{Å}$, 2.54_2Å , or 2.89Å , while the second-well separations are 4.46_2Å or 4.67Å . [Here and later, the subscript 2 tags all inter-layer separations; each such bond seen in projection is actually doubled, connecting up and down.] The Al-Al interaction is *repulsive* at the first-neighbor distances, but is weak at second-neighbor (or larger) separations. The strongest attraction is the deep Al-Co well at nearest-neighbor distance [$V_{\text{Al-Co}}(2.45) \approx -291\text{meV}$]; Al-Co is fairly attractive at second-neighbor distance too ($V_{\text{Al-Co}}(4.46) \approx -35\text{meV}$; Co-Co is also repulsive at first-neighbor distances, and more attractive than Al-Co at second-neighbor distance ($V_{\text{Co-Co}}(4.46) \approx -91\text{meV}$). In the interval 3-4 Å, all three interactions are rather repulsive. The general consequence of such potentials (in any Al-TM alloy with small enough TM fraction) is that TM atoms space themselves roughly equally so that each can have a coordination shell of Al atoms. In our rationalisation (below) of the order, we truncate the potentials at 5.1 Å: the Penrose structure emerges about as well in simulations with or without that truncation. Still, one should keep in mind that some “third neighbor” Al-Co or Co-Co interactions (around $R = 6\text{Å}$) are nearly as strong as the second-neighbor interactions that construct the matching rules.

In our Al-Co model, we can identify four stages of progressively greater order (and involving progressively smaller energy scales) upon cooling. The first two stages, at least, are the characteristic behaviour in *all* Al-TM decagonals simulated by our method [13, 14].

- 1 Organisation of Al coordination shells around Co atoms, along with a network of Al atoms alternating in layer and separated by a_R in projection, to form an HBS tiling with edge $a_R \approx 2.45\text{Å}$ (in projection).
- 2 Formation of a network of Co atoms, separated by $\tau a_R \approx 4.0\text{Å}$ (in projection) and alternating in layer. Every edge is divided (in projection) in the ratio $1 : \tau$ by an Al atom (in the layer which makes it roughly equidistant from each Co, right at the favorable Al-Co first-neighbor distances). The angles between edges are multiples of $2\pi/5$, and the ideal version of this network is a generalisation of the HBS tiling [19] which we’ll call the “HBS+” tiling. The HBS and Co-Co networks appear around $\beta = 5$; here most of space is filled by HBS tiles on both scales, but matching rules are mostly violated (Fig. 1(a), middle.) Normally the HBS tiling and the Co network form in tandem, but we get the former without the latter if (e.g.) we truncate the potentials at 3.5Å , or (of course) in the constrained simulation at high temperatures.
- 3 The “V-rule”: the two outer edges of a Thin rhombus (contained in the H or B tile) always fits against the concave corner between two Fat rhombi (belonging to the same B or S tile). Together the three rhombi constitute a Fat Hexagon, the diagonal of which is an edge of the Co-Co network (and when the V-rule is satisfied, *all* Co-Co edges are of this kind.)
- 4 The full Penrose matching rules.

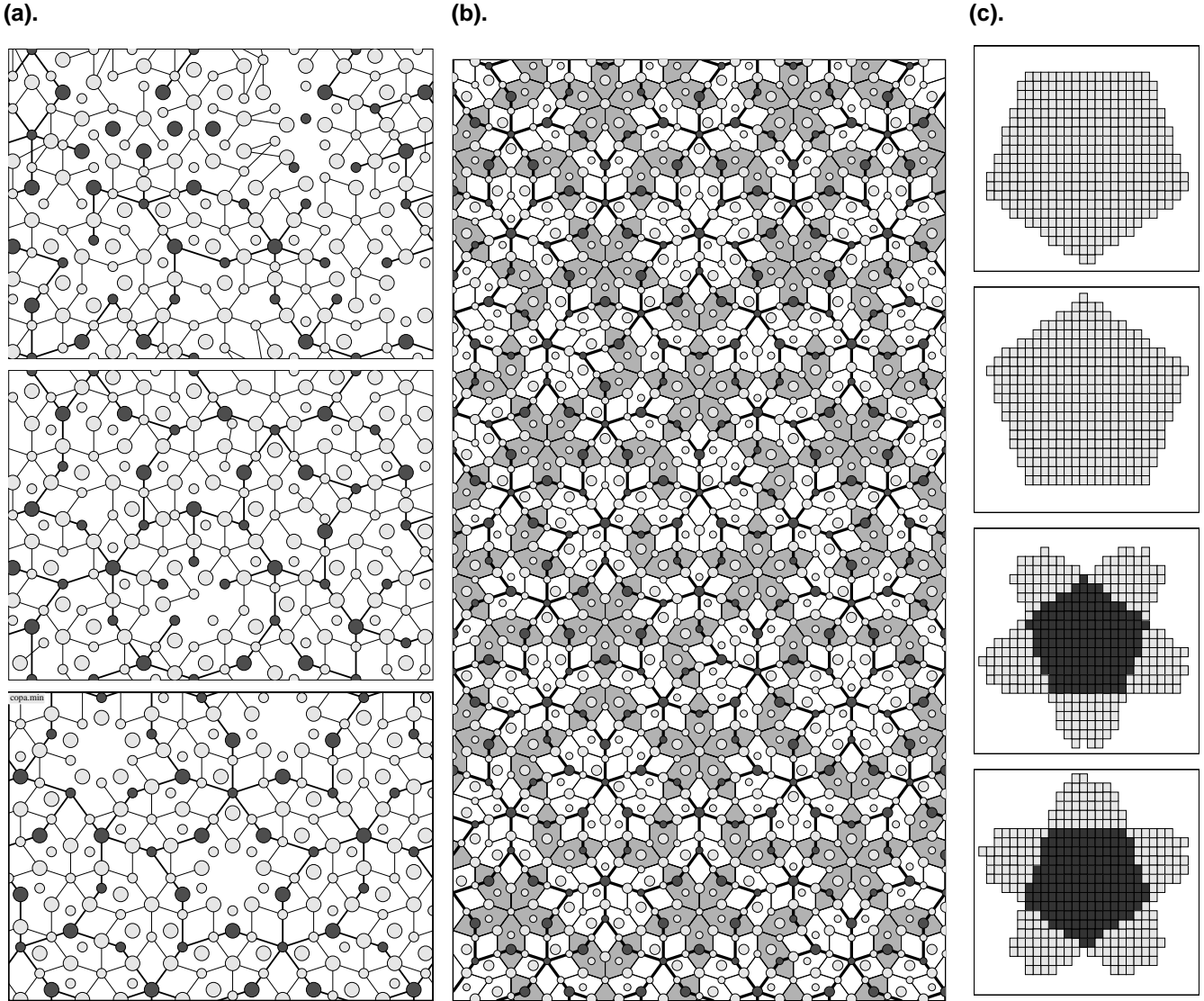


Figure 1. (a) Unconstrained simulation, in a cell $32.0 \times 23.3 \text{ \AA}$, with content $\text{Al}_{169}\text{Co}_{42}$. Co and Al atoms are shown by black and gray circles, with larger circles denoting the upper layer. Lines show Al-Al and Co-Co separations of the exact kind that will form edges of the respective ordered HBS tilings. Top to bottom: early, middle, and final stages in the ordering process. The first two are typical snapshots (taken during different parts of the $\beta = 4$ stage of a rapid cooling run with about 6000 trial swaps and 600 trial tile flips per candidate place); the (partial) “10 Å decagon” is characteristic of real Al-Co-Ni structures [?]. The last panel is the best energy seen (at $\beta = 12$) in the whole run: note how HBS tiles almost perfectly obey Penrose arrow rules. (b) A “constrained” simulation using identically decorated HBS tiles and a chemical potential of -1.8 eV for Al, in a cell $51.8 \times 98.5 \text{ \AA}$; temperature was lowered gradually from $\beta = 8$ to $\beta = 40$ during 5000 trial tile flips per flippable place (including rotations of Al within the Star tile). As a diagnostic of the Penrose order, note how the midlines of H tiles (shaded) form a τ^2 -inflated Penrose tiling. (c). Occupation domains formed by lifting the atoms to 4 layers in 5-dimensional space in the standard cut formalism; the Al atoms in layers ± 2 (top two panels) obviously form a perfect pentagon, modulo the pixel size; Co atoms appear with dark pixels in layers ± 1 (bottom two panels).

The 2.45-HBS tiling (stage 1) can be understood from first-neighbor Al-Al and Al-Co interactions. The Al network (with $R_{\text{Al-Al}} = 3.19_2 \text{ \AA}$ along edges, or 2.89 \AA on a Fat rhombus diagonal) is probably the only way to accommodate this number of Al atoms without hardcore violations. The arrangements of Al within the three HBS tiles seem to be the three best ways of maximizing the number of the (very strong) Al-Co nearest-neighbor bonds while minimizing Al-Al repulsions¹

Note that, in the HBS tiling, one can freely convert the combinations $\text{BB} \leftrightarrow \text{HS}$, but the Al content is respectively 4 and 3 on these tiles. Hence, if the HBS tiling is perfectly decorated, the Al density determines the comparative frequencies of the tiles: if δn_{Al} is the deviation of Al density from that in the Penrose

¹ S. Lim, M. Mihalkovič, and C. L. Henley, unpublished results.

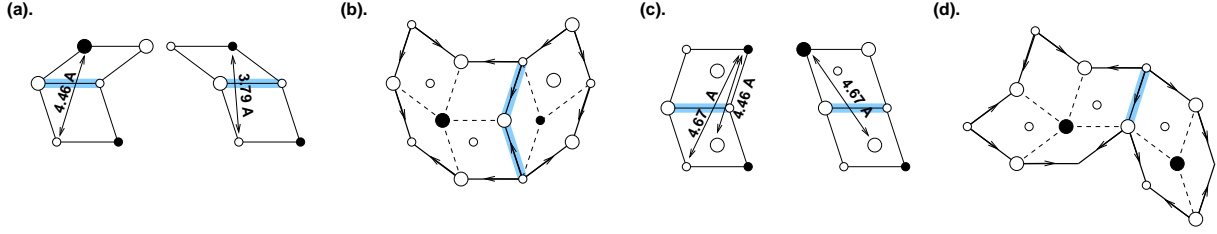


Figure 2. (a). Fat/Thin rhombus rule (adjoining along shaded edge); the correct relation (left) makes a favorable Al-Co bond at 4.46\AA . (b). Resulting “V” rule (the “V” is shaded). Penrose arrows are shown for the case of Boat and Hexagon tiles; internal edges shown dashed. (c). Fat/Fat rule: the correct relation (left) makes two additional 4.46\AA Al-Co separations, to the internal Al atoms. (d). Example of Fat/Fat rule on Boat and Hexagon.

tiling, then $\delta n_S = \delta n_H = -\delta n_B/2 = -\delta n_{A1}$.

The Co-Co network (Stage 2) is due to the strong Co-Co attraction at $R_{\text{Co-Co}} = 4.462\text{\AA}$ along the edge, or 4.67\AA across a Fat rhombus of the 4\AA tiling. Note that, if the “V-rule” is satisfied, the only tiles appearing in the “HBS+” tiling are H, B, S, plus P, the “pillow” tile¹

formed by ten Co atoms [one such tile is seen on the left edge of Fig. 1(a), middle panel.]

Also, an argument using the count of 4.67\AA bonds implies $\delta n'_S = 3\tau^2 \delta n_S$ where $\delta n'_S$ is the excess of the Star tile frequency (per 4\AA rhombus). Since the 4\AA HBS order implies that the number of 4.462\AA Co-Co bonds is a constant (for a given cell) and furthermore the V-rule implies the number of 4.67\AA Co-Co bonds is a constant (for a given Al content), the Co-Co energies cannot distinguish states that satisfy matching rule, so we will ignore them henceforth.

We now turn to effects that implement the Penrose matching rules on the edges of 2.45\AA -HBS tiles; in our tiling, the exterior edges of Fat and Thin rhombi are actually quite different, so we have in effect two (or more) flavors of arrow, and must check each combination of flavors. First, Thin-Thin rhombus edges (which in fact never occur in the Penrose tiling) would create a 2.89\AA Co-Co bond, so they are quite unfavorable (and excluded by the formation of the 4\AA Co-Co tiling). Second, as shown in Fig. 2(a), violating the arrows on a Thin/Fat shared edge removes the (attractive) 4.462\AA Al-Co bond and adds a (repulsive) 3.79\AA Al-Co bond, for a net cost of 80 meV. Satisfying Thin/Fat interactions maximally is equivalent to the V-rule [Fig. 2(b)], since the number of concave and convex V’s is exactly the same – provided the Al density (and hence the content of HBS tiles) is the same as in the Penrose tiling. (More generally, the number of convex V’s is invariant, but the density of concave V’s changes by $-\delta n_{A1}$.)

The only remaining case is a Fat-Fat shared edge. Assume the V-rule was satisfied: the Fat edges belonging to a concave “V” have all been paired with Thin rhombus edges, and the only remaining ones are the two sides of the Boat tile or of the Hexagon tile. In both cases, the Fat tile has an internal Al atom. Then, as shown in Fig. 2(c), violating the Fat/Fat matching rule loses 4.462\AA Al-Co bonds between the internal Al and the Co of the other tile, implementing the Fat/Fat matching rule and ensuring a Penrose tiling.²

In summary, the matching rules are mostly implemented by the Al-Co interaction at 4.462\AA . This was confirmed by counts of the energy contributions coming from each bond, as a function of temperature: over the temperature range when the matching rules are being established, the 4.462\AA Al-Co energy changed significantly, whereas other bonds’ contributions did not.

4 Discussion

We have exhibited, for the first time, a set of rather realistic interactions and a (nearly) realistic composition which organise into a Penrose tiling with matching rules. The rules are due to an interplay of relatively

¹ This tile was introduced and called “E” tile by M. Mihalkovič and M. Widom [20].

² Note the effective interactions can’t always be written in terms of adjoining tiles. In particular, at either tip of each Boat, if the matching rules are *both* satisfied (V-rule on one side, Fat/Fat on the other), then an additional (favorable) 4.67\AA Al-Co interaction is created between the Co atom on the V-rule side and the internal Al atom on the Fat/Fat side.

long-range interactions, especially Al-Co at $\sim 4.5 \text{ \AA}$, but often “conspiring” in that different interatomic terms contribute with the same sign to a tile-tile interaction. It was also important that the composition was tuned so as to enforce the Penrose-tiling ratio ($\sqrt{5} : 1$) between the numbers of Boat and Star tiles.

Our result opens more questions, both mathematical and physical. On the mathematical side, we do not yet have a rigorous proof that the Penrose structure is the (unique) optimum. For the “constrained” 2.45-HBS tiling, that seems quite feasible (with the potentials truncated at 5.1 \AA) Having done that, the more difficult half of the task would be proving the *unconstrained* structure is optimised in an HBS tiling (hence in a Penrose tiling); that calls for an assumption to limit the ensemble of structures to be compared with.

Physically, of course, one wonders what this says about real Al-TM systems. Our model system has an excess Al content and would be unstable to phase separation into non-quasicrystal phases. Compositions – outstandingly Al-Co-Ni – that do form equilibrium quasicrystals, are typically ternaries; they typically have variant decorations of the HBS tile interiors, and include additional objects (such as “ 8\AA Decagons” and “pentagonal bipyramids” in Co-rich Al-Co-Ni [14]). Due to this increased complexity, it seems likely that some of the inter-tile interactions would disfavor matching rules. Then the structure might deviate in places from the Penrose tiling at the 2.45 \AA scale, but might form super tilings at an inflated scale that do satisfy Penrose rules.

The simulation recipe we followed when modelling real decagonal quasicrystals [13, 14] had one more stage: relaxations and molecular dynamics (MD) simulations in which we let atoms depart from the discrete ideal sites. We have verified that our structure is robustly stable under MD, provided we maintain the $c = 4.08 \text{ \AA}$ stacking periodicity. However, the outstanding effect of relaxation in the real decagonals is “puckering” [15] whereby Al atoms bridging between Co atoms, as well as those interior to HBS tiles, rearrange their occupancy and displace from the planes, modulated with a doubled ($2c$) periodicity. This is likely to *strengthen* the “V-rule”, but might well flip the sign of the “Fat/Fat” matching rule.

It must also be observed that the same effects which implement matching rules in our toy composition, tended (in real compositions that we studied earlier) to favor combinations of tiles into supertiles that (within a supertile) looked like a Penrose inflation. Such structures showed many Penrose-like local patterns, and could be well approximated using Penrose tiling decorations, even if the ultimate ground state would be a non-Penrose packing of the supertiles.

5 Acknowledgements

This work was supported by U.S. DOE grant DE-FG02-89ER-45405; M.M. was also supported by Slovak research grants VEGA 2-5096/27 and APVV-0413-06.

References

- [1] R. Phillips and M. Widom, *J. Non-cryst. Solids* 153, 416 (1993)
- [2] J. Roth, R. Schilling, and H.-R. Trebin, *Phys. Rev. B* 41, 2735 (1990).
- [3] F. Lançon, L. Billard, and P. Chaudhari *Europhys. Lett.* 2 (1986) p. 625;
- [4] M. Widom, K. J. Strandburg, and R. H. Swendsen *Phys. Rev. Lett.* 58 (1987) p. 706.
- [5] A. Katz and D. Gratias, “Tilings and quasicrystals”, in *Lectures on Quasicrystals*, F. Hippert and D. Gratias, eds., Les Editions de Physique, Les Ulis, 1994, pp. 187-264.
- [6] V. Elser, *Phys. Rev. B* 32, 4892 (1985).
- [7] C. L. Henley, “Random tiling models”, in *Quasicrystals: The State of the Art*, P. J. Steinhardt and D. P. DiVincenzo, eds., World Scientific, Singapore, 1991, pp. 429-524.
- [8] J. E. S. Socolar and P. J. Steinhardt, *Phys. Rev. B* 34, 617 (1986)
- [9] M. de Boissieu, M. Boudard, B. Hennion et al., *Phys. Rev. Lett.* 75 (1995) p. 89.
- [10] F. Gähler, M. Baake, and M. Schlottmann, *Phys. Rev. B* 50, 12458 (1994).
- [11] L. S. Levitov, *Commun. Math. Phys.* 119, 627 (1988);
- [12] M. C. Shin and K. J. Strandburg, *J. Non-Cryst. Solids* 153, 253-257 (1993).
- [13] M. Mihalkovič, I. Al-Lehyani, E. Cockayne, et al., *Phys. Rev. B* 65, 104205 (2002).
- [14] N. Gu, M. Mihalkovič, and C. L. Henley, *Phil. Mag. Lett.* 87, 923 (2007).
- [15] N. Gu, C. L. Henley, and M. Mihalkovič, *Phil. Mag.* 86, 593 (2006).
- [16] E. Cockayne and M. Widom 1998, *Phil. Mag. A* 77, 593.
- [17] J. A. Moriarty and M. Widom 1997, *Phys. Rev. B* 56: 7905.
- [18] H.-C. Jeong and P. J. Steinhardt, *Phys. Rev. Lett.* 73, 1943 (1994).

- [19] C. L. Henley, “Cluster maximization, non-locality, and random tilings”, in *Quasicrystals*, S. Takeuchi and T. Fujiwara, eds., World Scientific, Singapore, 1998, p. 27.
- [20] M. Mihalkovič and M. Widom, *Phys. Rev. Lett.* 93, 095507 (2004).